



## FINITE ELEMENT SIMULATION OF SHORT CRACK BEHAVIOR UNDER THERMO-MECHANICAL LOADING CONDITIONS

Kai Bauerbach<sup>1</sup>, Jürgen Rudolph<sup>2</sup>, Michael Vormwald<sup>3</sup>

<sup>1</sup> Researcher, Materials Mechanics Group, TU Darmstadt, Germany (bauerbach@wm.tu-darmstadt.de)

<sup>2</sup> Expert and Senior Advisor, AREVA GmbH, Erlangen, Germany

<sup>3</sup> Professor, Materials Mechanics Group, TU Darmstadt, Germany

### ABSTRACT

In addition to structural loads such as internal pressure nuclear power plant components are generally also subjected to thermal cyclic loading conditions. The transient cyclic nature of these events causes stress-strain hysteresis loops which are considered to be fatigue relevant events. To consider the impact of such events for the fatigue assessment a short crack approach using a J integral based damage parameter is utilized.

The local stresses and strains are computed from a two step FE Analysis. All calculations are based on the component example of a thick walled tube. In a transient thermal analysis the temperature solution is obtained using temperature dependant material parameters. The mechanical temperature dependent material behavior is implemented using a Chaboche type elastic plastic material model for a typical stabilized austenitic stainless steel. Appropriate material parameter identification relies on systematic experiments.

The loading conditions are taken from sample low cycle temperature transients comparable to those arising during the operation of nuclear power plants.

To calculate the solution for a cracked configuration a short crack in axial direction is introduced into the wall of the tube. The algorithm uses a node release technique as well as contact elements along the crack flanks to describe different states of a short crack configuration as well as opening and closure effects. The results are interpreted for fatigue assessment using a damage parameter based on the cyclic effective J integral. The values are calculated based on the results of the FE Analysis.

### INTRODUCTION

Damage and failure prevention is a major responsibility during operation of complex systems such as nuclear power plants. Fatigue due to cyclic thermo-mechanical loading constitutes a major ageing relevant potential damage mechanism. In practice the identification of such events includes fatigue monitoring allowing reviewing and optimization of the operating modes. For nuclear power plants the design codes (ASME, KTA, RCC-M) guide the way to perform the proofs of fatigue strength.

After the relevant fatigue events can be identified it is essential to perform a damage assessment procedure to evaluate the severity of the identified event. For a more comprehensive understanding of component failure and fatigue life a deeper knowledge of the mechanisms and driving forces behind those phenomena is essential.

The extension of the short crack approach as it has been established by Döring et al. (2006) for isothermal cases is extended into the field of non-isothermal thermal cyclic loading. This requires an extension of known crack parameters as the original isothermal formulation suffers massive drawbacks when applied to cases of thermal cyclic loading conditions.

In the presented framework the crack tip opening displacement is assumed to be the temperature independent crack driving force. The numerical results show that this value can also be determined in terms of a cyclic J integral allowing a subsequent damage assessment in form of a crack growth analysis using a crack growth law.

## DAMAGE ASSESSMENT AND FE SIMULATION

The damage assessment follows the routine described in Bauerbach et al. (2009). The results of a Finite Element Analysis are evaluated in terms of the cyclic J integral. As the approach only considers damage to occur when the flanks of a short crack are separated it is necessary to consider the influence of crack closure.

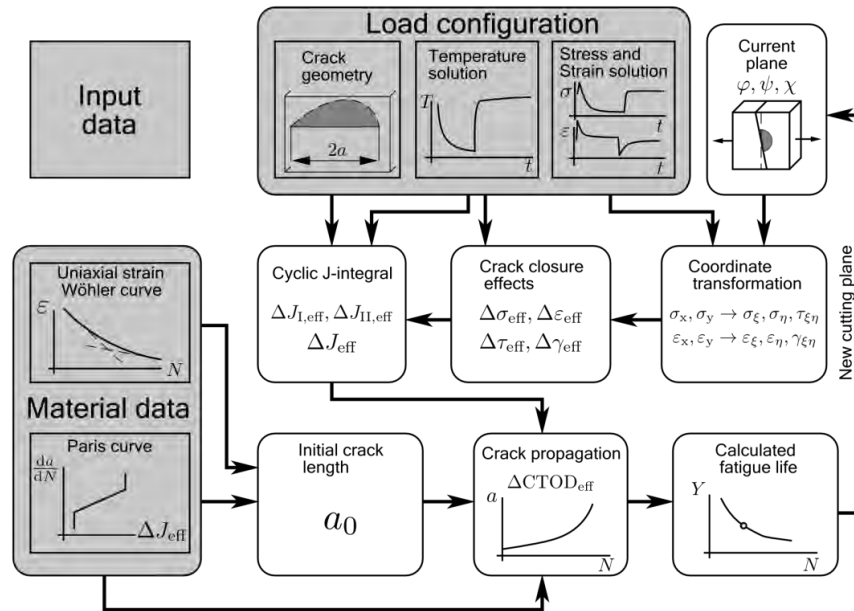


Figure 1. Damage assessment routine overview

In this paper we take a detailed look into the question of opening and closure of a short crack subjected to thermal cyclic loading conditions as well as the assessment routine that follows the FE simulation of thermal cycles in terms of a crack tip parameter.

The model used for the numerical simulations represents a thick walled tube similar to the system used in Bauerbach et al. (2009). The inner diameter of the tube is 190 mm with a wall thickness of 40 mm. The considerations in this paper however require a cross section of the tube to be modeled. Working with a cross section model reduces the computational effort and allows for an easy introduction of a short crack into the wall. Figure 2 depicts the upper half of the cross section of the tube. In the same manner as described in Rudolph et al. (2010) the calculations are performed using a torus with a large primary radius to model a tube of arbitrary length. Given that the distance between the center of the torus and the center of the cross section is large when compared to the diameter of the cross section the use of this axial symmetry is a legitimate way to model a tube of arbitrary length. The inside wall on the right side of the model is meshed considerably finer than the rest of the cross section. Figure 3 shows the mesh refinement. The element edges in this part of the mesh have a length of 10  $\mu\text{m}$ .

Table 1. Temperature dependant material parameters for the thermal transient calculation

	20 °C	100 °C	200 °C	300 °C	400 °C
Thermal conductivity $\frac{\text{N}}{\text{sK}}$	15.0	16.0	17.0	19.0	20.0
Heat capacity in $10^9 \frac{\text{mm}^2}{\text{Ks}^2}$	0.47	0.47	0.49	0.50	0.52
Density in $10^{-9} \frac{\text{N}}{\text{s}^2\text{mm}^4}$			7.93		

All material parameters for the thermal calculation are taken from the KTA and given in Table 1 for five distinct temperatures. The density is assumed to be constant over the whole temperature range.

The stress strain solution is obtained from a unidirectionally coupled field FE analysis. This analysis procedure consists of two FE simulations. In the first a thermal transient calculation is performed. This simulation uses thermal elements with the temperature as the nodal degree of freedom (DOF). The boundary conditions for this analysis step are given in form of a temperature transient that defines the bulk temperature of the medium running through the tube as well as the heat transfer coefficient. The result of this simulation is the temperature profile for the given temperature transient (see Figure 4 for a sample transient). This temperature profile consists of the thermal field solution for all nodes for the transient's duration.

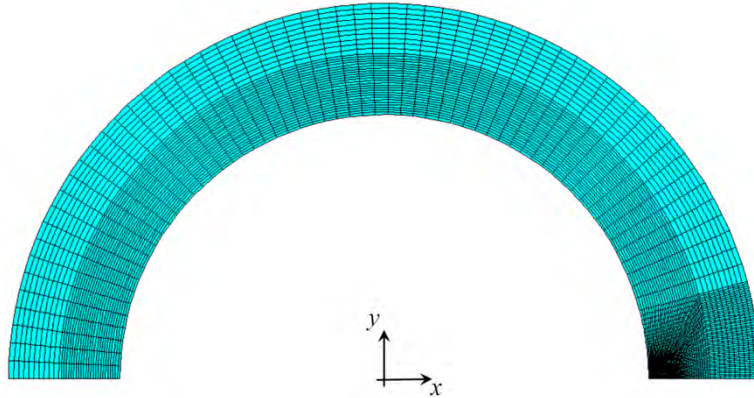


Figure 2. Mesh and model of the upper half of the tube's cross section

In the second simulation step this temperature profile is applied repeatedly as a loading information together with a constant pressure on the inside wall of the tube. As an additional displacement boundary condition to the above described rotational symmetry the nodes at  $y = 0$  are held in  $y$  direction to properly utilize the half symmetry of the tube's cross section.

The elastic plastic stress strain behavior of the material is represented using the material model described by Chaboche (1989) as it is native to the FE Software ANSYS<sup>®</sup>. The material parameters for the structural calculation are based on the report by Hertel et al. (2007). The cyclic stress strain curves for the material 1.4550 are given for three temperatures to properly consider the temperature's influence on the stress strain behavior for the structural calculation.

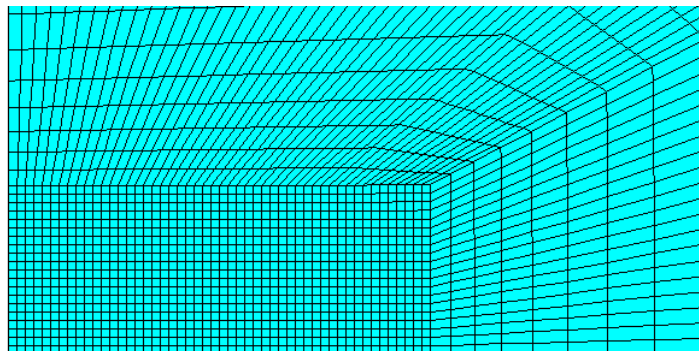


Figure 3. Detail view of the mesh on the inside wall on the right side

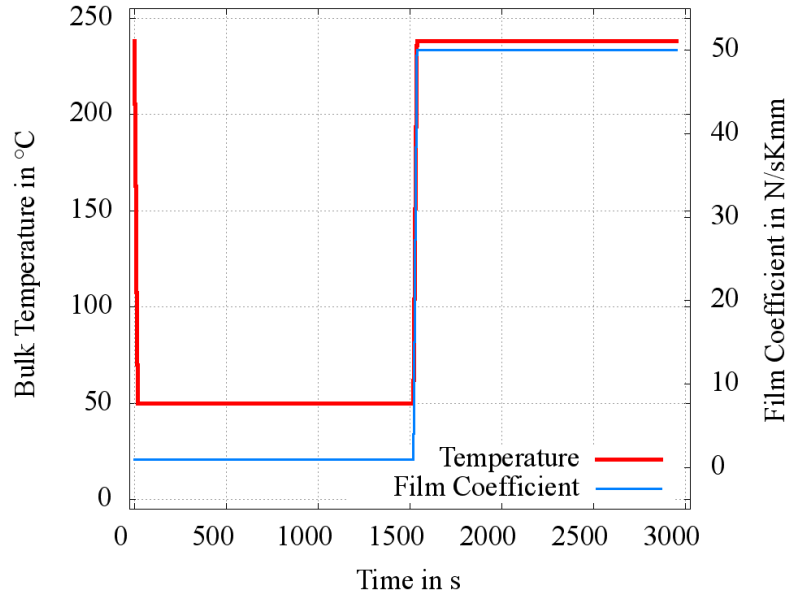


Figure 4. Sample temperature transient for the thermal transient FE analysis step

For this second calculation the previously calculated temperature profile is applied for a total of 10 times. This number of cycles is chosen to obtain a stabilized stress-strain hysteresis. The results of the simulation reflect this stabilized state of the circumferential hysteresis loops along the inside wall. The temperature transients are defined appropriately to ensure that the temperature field at the end of one thermal cycle is the same uniform temperature distribution as the initial thermal state. As this calculation assumes a unidirectional coupling of the field solutions the results of the structural simulations do not have any impact on the thermal simulation.

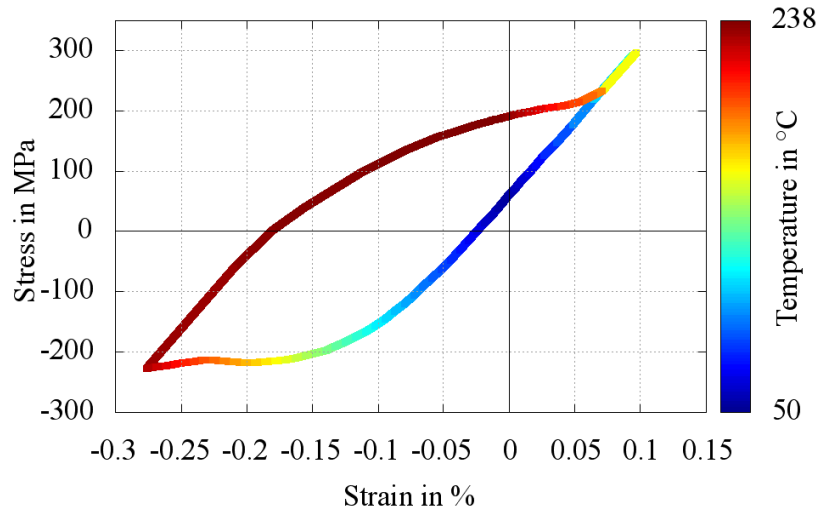


Figure 5. Reference hysteresis loop in circumferential direction on the right side of the inside wall

For all further considerations only the stress, strain and temperature results on the right side of the inside wall are of importance. For the last of the 10 thermal cycles this data is saved as a reference hysteresis loop.

## CRACK OPENING AND CLOSURE

To consider the effects of opening and closure of a short crack an additional FE simulation has been performed. The third simulation step is again a structural simulation. For this step again the previously calculated temperature profile is applied repeatedly to simulate the thermal cyclic loading conditions. Additionally this simulation employs a nodal release scheme to model the growth of a short crack into the wall on the right side of the above described model. It is important to note that in the calculations no real crack growth is considered. The algorithm does not contain a specific loading dependant criterion to propagate the crack. Instead the nodal release is performed after a fixed number of cycles. To consider crack closure contact elements are introduced into the model.

The contact elements are applied to all nodes on the prescribed crack path  $x > 0; y = 0$ . Adding appropriate Target Elements along the same coordinate line prevents the nodes on the crack flanks to be displaced below the  $y = 0$  line of the model which would result in a self penetration of the crack flanks when considering the half-symmetry of the cross section. Note that here only one crack flank is modeled as the other will behave symmetrically.

Starting with the very first node on the inside wall the boundary conditions in  $y$  direction are deleted. The temperature profile and the internal pressure are then applied for a block of 10 cycles. After this block another nodal boundary condition is released. This procedure is repeated for a total of 20 Block resulting in 200 cycles for crack length configurations from  $10\mu\text{m}$  to  $200\mu\text{m}$ .

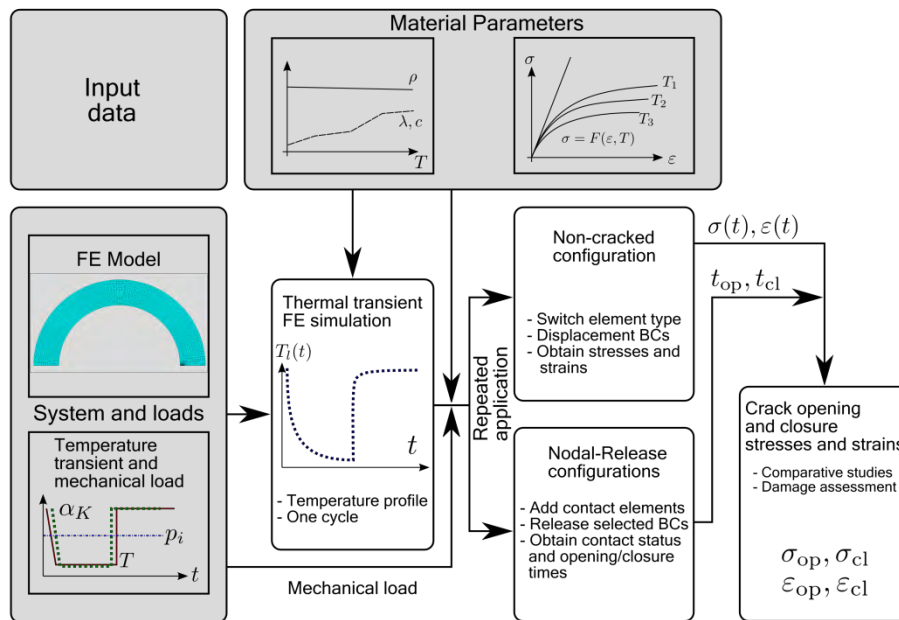


Figure 6. Schematics of the procedure to obtain opening and closure stresses and strains

Using this approach ensures that the elements on the crack flank retain the plastic strain they experienced when those elements were previously located at the crack tip and therefore ensures crack configurations as close as possible to a crack that results from the actual growth of a crack into the tube's wall.

For each of these crack configurations the opening and closure of the nodes on the crack flank is extracted for the last cycle in each block. It is assumed that after 10 cycles the stress strain field as well as the deformation cycle in the vicinity of the crack has reached a quasi stabilized state. The crack is considered open as long as all nodes on the crack flank give a contact status 'open'. As soon as the first

contact status changes to ‘closed’ the crack is considered closed. The according time steps of the calculation are then considered to be the points of crack opening and closure. Transferring the time of these data points back to the corresponding points in reference hysteresis allows determining the stresses and strains when a crack of the length given by the crack configuration would open or close. This is done by taking the point of time in the thermal cycle when opening or closure occur and then obtaining the stress and strain from the reference hysteresis loop obtained from the non-cracked simulation.

For isothermal cases the equations by Newman (1984) are widely accepted to calculate the crack opening stress for a hysteresis loop. However, numerical investigations shown in Rudolph et al. (2010) clearly indicate that the results obtained from a Newman approach for non-isothermal loading conditions are not in agreement with the results obtained from FE analyses.

## CALCULATION OF THE CYCLIC J INTEGRAL

In the context of linear elastic fracture mechanics the near-field is characterized by the stress intensity factors  $K_i$ . When considering elastic-plastic material behavior the J-integral is commonly used as the relevant Parameter. It was originally formulated by Rice (1968) and has been modified by Dowling and Begley (1976) as well as Wüthrich (1982) to be applicable for cyclic loading cases.

The original definition of the J integral according to Rice is

$$J = \int_{\Gamma} \left( W dy - t_i \frac{\partial u_i}{\partial x} ds \right) \quad (1)$$

Where  $u_i$  is the displacement vector and the strain energy density is

$$W = \int_0^{\varepsilon_{ij}} \sigma_{ij} \varepsilon_{ij} \quad (2)$$

The path integration is performed along the closed contour  $\Gamma$  around the crack tip. The stress vector  $t_i$  is calculated from the stress tensor  $\sigma_{ij}$  and the vector  $n_j$  normal to  $\Gamma$ . The J integral is considered to be path independent. The value calculated is invariant with respect to the path around the crack tip.

For the application to cyclic loading cases we define the stress-strain state at load reversal as a reference state 0 and replace all variables in (1) with parameters that are related to this state

$$\begin{aligned} \Delta\sigma_{ij} &= \sigma_{ij} - \sigma_{ij}^0 \\ \Delta\varepsilon_{ij} &= \varepsilon_{ij} - \varepsilon_{ij}^0 \\ \Delta u_i &= u_i - u_i^0 \end{aligned} \quad (3)$$

The cyclic J integral then becomes

$$\Delta J = \int_{\Gamma} \int_0^{\Delta\varepsilon_{ij}} \Delta\sigma_{ij} d\Delta\varepsilon_{ij} dy - \int_{\Gamma} \Delta\sigma_{ij} n_j \frac{\partial \Delta u_i}{\partial x} ds \quad (4)$$

It is important to note that  $\Delta J$  does not denote the range of the J integral. The  $\Delta$  denotes that two stress-strain states on the descending hysteresis branch are linked according to Equation (3). Equation (4) is evaluated from the point of loading reversal to a defined end point. The evaluation is performed on the descending hysteresis branch. This ensures that all elements involved in the calculation follow the same direction in their deformation see Vormwald (1989). To ensure path independence the crack flanks must be free of surface loads and may not touch or overlap.

Due to the nature of the temperature cycle with a temperature field solution that varies in time and leads to steep temperature gradients in the vicinity of the crack the evaluation of the cyclic J integral according to Equation (4) exhibits severe path dependencies, see Bauerbach and Vormwald (2013). To circumvent the problem of path dependant solutions of the cyclic J integral the analysis has been modified according to Aoki et al. (1980) and Kishimoto et al. (1982) respectively to incorporate the influence of the thermal strains.

An extension of the J integral by these authors to consider additional thermal loading is

$$\hat{f} = - \int_{\Gamma} t_i \frac{\partial u_i}{\partial x} ds + \iint_A \sigma_{ij} \frac{\partial \hat{\varepsilon}_{ij}}{\partial x} dA \quad (5)$$

with the total strain being the sum of elastic, plastic and thermal strains.

$$\hat{\varepsilon}_{ij} = \varepsilon_{ij}^{el} + \varepsilon_{ij}^{pl} + \varepsilon_{ij}^{th} = \varepsilon_{ij}^{mech} + \varepsilon_{ij}^{th} \quad (6)$$

Deriving a new formulation for the cyclic J integral based on Equation (5) follows the same steps as described for Equations (3) and (4). Separation of the mechanical and thermal strains allows transforming the area integral in Equation (5) into a mixed area and line integral. Considering that the thermal strains are always volumetric allows omitting the deviatoric part of the calculation for the thermal strains.

$$\Delta \hat{f} = \int_{\Gamma} \int_0^{\Delta \varepsilon_{ij}} \Delta \sigma_{ij} d\Delta \varepsilon_{ij}^{mech} dy - \int_{\Gamma} \Delta \sigma_{ij} n_j \frac{\partial \Delta u_i}{\partial x} ds + \iint_A \alpha \Delta \sigma_{ii} \frac{\partial \Delta \theta}{\partial x} dA \quad (6)$$

The temperature  $\Delta \theta$  is then the temperature difference of the reference state and the current temperature for each evaluated time step. In Equation (6)  $\alpha$  is the thermal expansion coefficient. An analogous formula for the J integral without the additionally denoted  $\Delta$  can be found in Kuna (2008) also referencing Aoki et al. (1982). Kuna mentions that determining the temperature derivative from the nodal temperatures leads to the same solution quality as the strains. The area integral in the above equation arises from the thermal dependence of the strain energy density. In this case, the stresses together with the thermal strains contribute a non-negligible term to the strain energy density. Therefore, these terms have to be considered in the above integration.

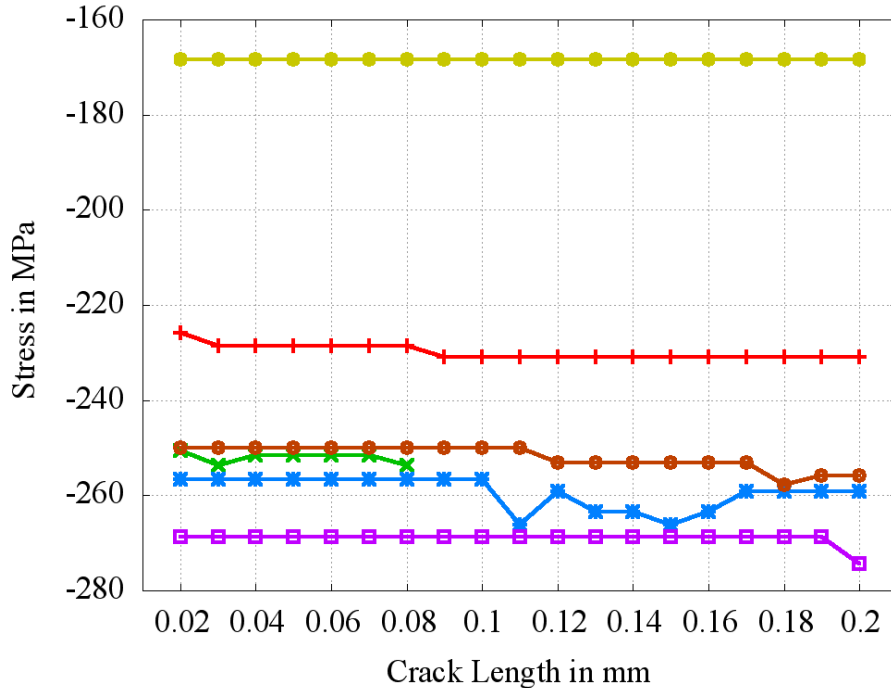


Figure 7. Development of the crack closure stress over crack length for different temperature transients

The algorithm for the first 2 integrals in Equation (6) has been implemented and tested by Hertel et al. (2004) for non-proportional loading cases.

For the evaluation of the additional area integration term the algorithm determines the temperature range at each node of all elements in the integration area. The spatial derivative is taken assuming the temperature field within each element can be described in terms of the FE shape functions. As a last step a Gauss integration scheme is used to calculate the area integral contribution for each

element. For a comprehensive description of the numerical procedure to obtain the values for  $\Delta\hat{J}$  see Bauerbach and Vormwald (2013).

As the numerical evaluation of Equation (6) is performed for a given strain range from 0 to  $\Delta\varepsilon_{ij}$  the starting and ending load steps for this procedure need to be defined. The calculation starts at the point of maximum crack tip opening displacement and ends when the first node on the crack flank changes its contact status to 'closed'.

## RESULTS

The results for the crack closure stresses are the stresses taken from the non-cracked configuration. These are extracted for respective load step of crack closure in the cracked configuration. As the point of crack closure is the relevant ending point of the evaluation of Equation (6) the closure stresses are given in Figure 7. The figure clearly shows that the load step of crack closure does not change considerably for different crack length scenarios.

The values for the modified cyclic J integral are calculated based the FE Analysis on the different 'cracked' configurations. For the last cycle in each block of 10 cycles the value is calculated. The value for the crack tip opening displacement  $\Delta\text{CTOD}$  is taken as the maximum value of the vertical displacement of the node on the crack flank closest to the tip.

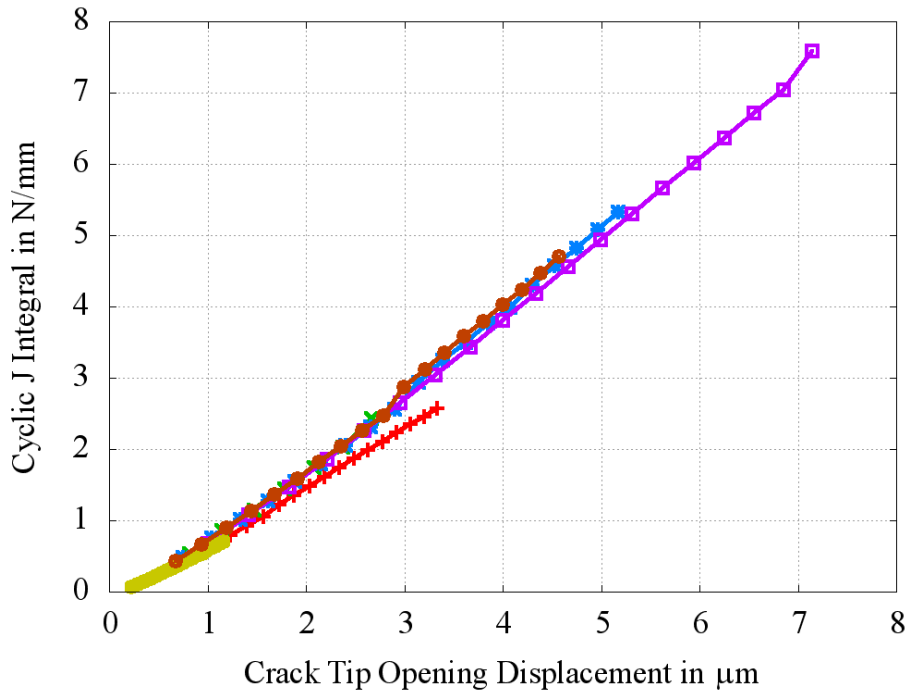


Figure 8. Values of the cyclic J integral via the modified algorithm versus  $\Delta\text{CTOD}$  for different temperature transients

Figure 8 indicates a quasi-linear relation for all analyzed temperature transients between the cyclic J integral and the crack tip opening displacement values.

To obtain a value that could represent a damage parameter Figure 9 shows the development over the crack length. This plot indicates a characteristic damage parameter value that seems to be practically independent of the crack length and can be determined by either the modified cyclic J integral or the crack tip opening displacement. This relation has been assumed by Schmidt et al. (2002). In this publication the hypothesis has been presented and verified that the crack growth law is independent of the temperature if

expressed in terms of the cyclic crack tip opening displacement  $\Delta CTOD$ . As our results indicate the linear relation between the two the formulation of a temperature independent crack growth law in terms of a modified cyclic J integral as given by Equation (6) appears valid.

Within the framework of our research project the analyses presented here have also been performed using an Ohno/Wang material model as described and implemented by Willuweit (2009). The preliminary results obtained from these simulations strongly support our findings.

## ACKNOWLEDGEMENT

This work is part of the R&D project “Simulation and characterization of the material state of components subjected to thermal cyclic loading conditions”. This project is co-financed and accompanied by the German Ministry of Education and Research (BMBF), by VGB PowerTech technical association of companies of power plant operators and manufacturers. This cooperation is gratefully acknowledged.

The German Ministry of Education and Research sponsors this project under the support code 02NUK009D. The authors are responsible for the contents of this paper.

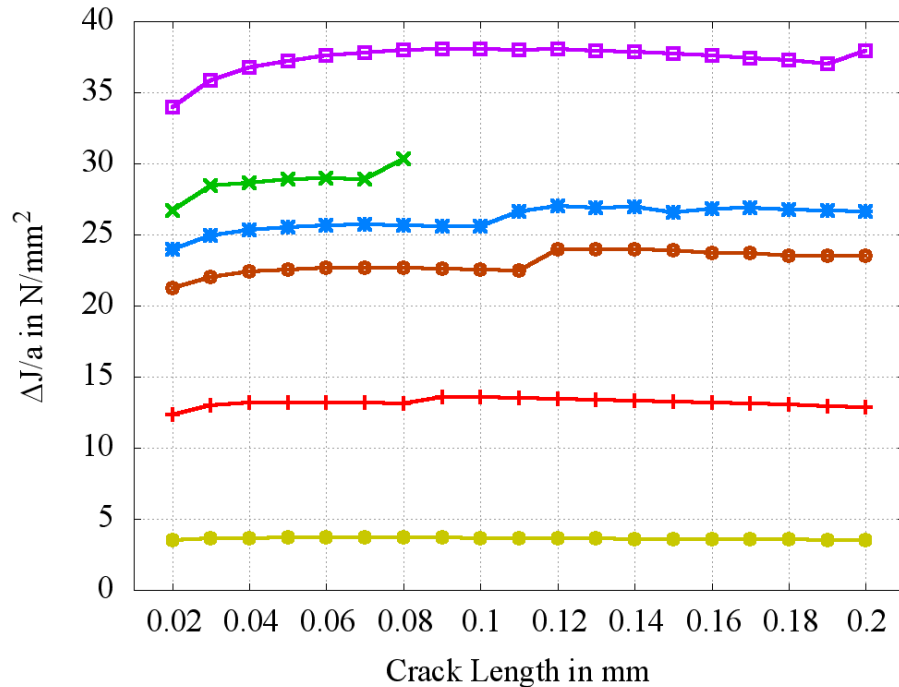


Figure 9. Damage Parameter development versus crack configurations

## REFERENCES

- Aoki, S, Kishimoto, K., Sakata, M. (1980) “Elastic-Plastic Analysis of crack in thermally loaded Structures”, Engineering Fracture Mechanics 13(4), 841-850
- ASME, (1969) Criteria of the ASME Boiler and Pressure Vessel Code for Design by Analysis in Sections III and VIII, Division 2.
- ASME Boiler & Pressure Vessel Code, (2007). Section III Division 1 – Subsection NB: Class 1 Components; Rules for the Construction of Nuclear Power Plant Components

- Bauerbach, K., Vormwald, M., Rudolph, J. (2009) "Fatigue assessment of nuclear power plant components subjected to thermal cyclic loading", PVP2009-77450, Proceedings of PVP2009, 2009 ASME Pressure Vessels and Piping Division Conference July 26-30, 2009, Prague, Czech Republic
- Bauerbach, K., Vormwald, M. (2013) "Zur Auswertung des zyklischen J-Integrals  $\Delta J$  bei temperaturabhängigem elastisch-plastischen Materialverhalten unter nicht-isothermen Bedingungen" 45. Tagung des DVM-Arbeitskreises Bruchvorgänge, DVM, Berlin, February 19-20 2013, pp 13-25
- Chaboche, J. (1989) "Constitutive equations for cyclic plasticity and cyclic viskoplasticity", International Journal of Plasticity, 5, pp. 247–302
- Dowling, N. E., Begley, J. A. (1976) "Fatigue crack growth during gross plasticity and the J-integral", ASTM590, 82-103
- Dowling, N. E. (2003) "Local Strain approach to Fatigue" Comprehensive Structural Integrity, Elsevier, 4, pp. 77–94.
- Döring, R., Hoffmeyer, J., Seeger, T., and Vormwald, M., (2006) "Short fatigue crack growth under nonproportional multiaxial elastic-plastic strains", International Journal of Fatigue, 28, pp. 972–982
- Hertel, O., Döring, R. and Vormwald, M. (2004) "Cyclic J-Integral under Nonproportional Loading", Proceedings of the 7th International Conference on Biaxial/Multiaxial Fatigue & Fracture, 513-518
- O.Hertel, O. and Vormwald, M. (2007) „Zyklische Werkstoffversuche und Parameteridentifikation für die Plastizitätsmodelle nach Chaboche und Ohno-Wang“, Bericht FI-145/2007, Institut für Stahlbau und Werkstoffmechanik TU Darmstadt.
- KTA 3201.1 (1998) "Components of the Reactor Coolant Pressure Boundary of Light Water Reactors Part 1: Materials and Product Forms", Kerntechnischer Ausschuss
- KTA 3201.2 (1996) "Components of the Reactor Coolant Pressure Boundary of light Water Reactors Part 2: Design and Analysis", Kerntechnischer Ausschuss
- Kuna, M. (2008) "Numerische Beanspruchungsanalyse von Rissen – Finite Elemente in der Bruchmechanik", Vieweg+Teubner
- Kishimoto, K., Aoki, S., Sakata, M. (1982) "On the Path Independent Integral  $J$ ", Engineering Fracture Mechanics Vol. 16, No. 3 , 405-413
- Newman Jr., J. C. (1984) "A crack opening stress equation for fatigue crack growth". Int. J. Fract.(24), pp. 131–R135
- Rudolph, J., Bauerbach, K., Vormwald, M. (2010) "Numerical Investigations of Phenomena Caused by the Closure and Growth Behavior of Short Cracks Under Thermal Cyclic Loading", Proceedings of the ANSYS Conference & 28th CADFEM Users' Meeting, Leipzig, November 3-5, 2010 Eurogress Aachen
- RCC-M Edition, 2000. Class 1 Components: Design and Construction Rules for Mechanical Components.
- J. R. Rice: A Path Independent Integral and the Approximate Analysis of Stress Concentration Factors, Journal of Applied Mechanics 35 (1968) 379-386
- Seeger, T. (1988). Werkstoffmechanisches Konzept der Dauer- und Zeitfestigkeit , Bericht FF-3/1988 ed. Fachgebiet Werkstoffmechanik, Technische Hochschule Darmstadt.
- Schmidt, W., Mohrmann, R., Riedel, R., Dietsche, H., Fischersworing-Bunk, F. (2002) "Modelling of the fatigue life of automobile exhaust components". Fatigue 2002, Stockholm, pp. 781–788
- Vormwald, M. (1989) „Anrißlebensdauervorhersage auf Basis der Schwingbruchmechanik für kurze Risse“, Heft 47, Institut für Stahlbau und Werkstoffmechanik, TU Darmstadt
- Willuweit, A. (2009) „Implementierung der Materialmodelle von Chaboche und Ohno/Wang in ANSYS zur Simulation von mechanisch- und thermomechanisch induzierter fortschreitender plastischer Deformation (Ratcheting)“, ANSYS Conference & 27. CADFEM User's Meeting, Leipzig
- Wüthrich, C. (1982) "The Extension of the J-Integral Concept to fatigue Cracks", Int Journal of Fracture 20, R35-R37